



OPEN

Witness of non-Markovian dynamics based on Bhattacharyya quantum distance

Seyed Mohammad Hosseiny ✉, Jamileh Seyed-Yazdi ✉ & Milad Norouzi 

Non-Markovian effects due to quantum memory in the dynamics of open systems typically correspond to information backflows from the surrounding environment to the system. We propose a witness to quantify the non-Markovianity of quantum evolutions using the Bhattacharyya distance (BD), a specific quantum statistical distance. This witness has the advantage of not requiring the calculation of the evolved density matrix and only computes through the initial and final states of the system, therefore leading to the improvement of quantum metrology. It means that we calculate the quantum angle between two states to detect non-Markovian effects. This proposal is investigated by considering several instances of open quantum systems, such as two and three-level atoms interacting in single and two-mode fields, respectively, and two effective two-level atoms interacting locally with two independent environments. We demonstrate that the suggested BD-based non-Markovianity witness identifies memory effects, consistent with well-established witnesses based on Bures distance, quantum Fisher information, and Hilbert-Schmidt speed, showing sensitivity to information backflows.

Keywords Non-Markovianity witness, Quantum statistical distance, Bhattacharyya distance, Memory effects

Abbreviations

CP	Complete positivity
BD	Bhattacharyya distance
TD	Trace distance
HSS	Hilbert-Schmidt speed
CSS	Classical statistical speed
POVM	Positive operator-valued measure
QSS	Quantum statistical speed
BT	Bhattacharyya distance threshold

Quantum system's interaction with their surrounding environment causes the exchange of information, potentially resulting in energy dissipation and the loss of quantum coherence^{1–6}. However, the process does not need to be monotonic as the quantum system may temporarily regain some of the lost energy or information due to memory effects during the evolution^{7–20}. This dynamic behavior, known as non-Markovianity, can manifest in different quantum information tasks such as teleportation involving mixed states²¹, boosting channel capacity in quantum systems²², optimal entanglement protocols^{23–25}, and extracting work from an Otto cycle²⁶.

In the context of information flow in open quantum systems, the dynamics involving the system's interaction with its environment are divided into two categories^{8,27,28}: Markovian and non-Markovian dynamics. If information flows continuously from the system to the surrounding environment, it is referred to as Markovian dynamics. Conversely, information backflow to the system from the environment at some time intervals due to quantum memory effects is known as non-Markovian dynamics.

Research on the non-Markovianity of dynamics in quantum systems has been extensively studied^{8,9,29,30}. Some important witnesses of non-Markovianity effects have been proposed based on different dynamical metrics such as quantum mutual information³¹, the flow of quantum Fisher information (QFI)^{32,33}, and simple tool of Hilbert-Schmidt speed (HSS)³⁴. Another approach is to probe temporary increases in the entanglement shared between the open quantum system and an isolated ancilla via measuring the deviation from complete positivity (CP) divisibility of the dynamical map that represents the system's evolution, which was first suggested

Physics Department, Faculty of Science, Vali-e-Asr University of Rafsanjan, Rafsanjan, Iran. ✉ email: hosseinyismohammad@gmail.com; j.seyed Yazdi@gmail.com

by Rivas et al.³⁵. The next key approach relies on assessing the distinguishability of two optimal initial states evolving through the same quantum channel or resource and investigating any nonmonotonicity (backflows of information) is quantified by the trace distance (TD) as first proposed by Breuer et al.^{27,36}. Moreover, negative time-dependent decoherence rates in the standard shape of the master equation³⁷, local quantum uncertainty³⁸, coherence^{39,40}, fidelity of the quantum states^{41,42}, channel capacities⁴³, quantum interferometric power^{44–46}, Choi states⁴⁷, changing in the volume of the set of accessible states in the evolved system⁴⁸, correlation measures⁴⁹, spectral analysis⁵⁰, quantum evolution speedup^{51–53}, and entropy production rates⁵⁴. This array of witnesses and approaches highlights the diverse nature of non-Markovian behavior, making it challenging to attribute to a single system-environment interaction feature, hindering its characterization with a single tool for this phenomenon. Therefore, searching for new witnesses to detect non-Markovianity effects in various situations within open quantum systems is beneficial.

In this article, we aim to introduce a method for witnessing and measuring non-Markovianity using the Bhattacharyya distance (BD)^{55,56}, which is a particular case of the quantum statistical distance⁵⁷. The advantage of this witness is a simple form for computation, as it does not require the calculation of the evolved density matrix. It only computes through the initial and final states of the system, thereby leading to an improvement in quantum metrology. Moreover, we examine the BD-based non-Markovianity witness detects memory effects, in total agreement with witnesses based on the QFI, Bures distance, and HSS therefore identifying system-environment information backflows. This proposal is studied based on the two open quantum systems including the two and three-level atoms interacting with single and two-mode fields, respectively, and two effective two-level atoms interacting locally with two independent environments.

The article is structured as follows: In section “Preliminaries”, the preliminaries of non-Markovianity witnesses are discussed, and the suggested BD witness is introduced. Additionally, in section “The physical models”, the theoretical models are presented. Finally, in section “Discussion and results”, we outline the key discoveries and discussions such that the sensitivity of this measure for identifying memory effects is studied.

Preliminaries

Non-Markovianity witnesses

Quantum Fisher information (QFI)

One of the most crucial witnesses of non-Markovianity is quantum Fisher information (QFI)³². The QFI can serve as a tool for quantum estimation of the desired parameter ϑ . For instance, we can utilize the QFI to estimate phase in an open quantum system. Considering the quantum Cramer-Rao bound⁵⁸, one can obtain the smallest resolvable change in the parameter ϑ by

$$\delta\vartheta = \left(1/\sqrt{\mathcal{F}_\vartheta}\right), \quad (1)$$

where \mathcal{F}_ϑ represents the QFI and for pure states can be simply defined by⁵⁹

$$\mathcal{F}_\vartheta = 4[\langle\dot{\psi}|\dot{\psi}\rangle - |\langle\dot{\psi}|\psi\rangle|^2]. \quad (2)$$

in which $|\dot{\psi}\rangle = (\partial/\partial\vartheta)|\psi\rangle$. The theory of quantum estimation suggests that an increase in QFI signifies an improvement in the optimal accuracy of estimation. Therefore, QFI is a useful measure of the maximum information on parameter ϑ that can be obtained from a measurement process.

Hilbert-Schmidt speed (HSS)

Hilbert-Schmidt speed (HSS) is recognized as another potent tool for improving quantum parameter estimation in quantum information theory. As suggested in^{34,60}, the HSS can be utilized as a non-Markovianity witness that identifies memory effects.

To introduce the HSS, we can consider the Hellinger distance criteria $d(p, q)$, defined by $[d(p, q)]^2 = \frac{1}{2} \sum_x |p_x - q_x|^2$ ⁵⁷, such that $p = \{p_x\}_x$ and $q = \{q_x\}_x$ represent the probability distributions corresponding to the desired parameter ϑ , which results in characterizing the classical statistical speed (CSS) $s[p(\vartheta_0)] = \frac{d}{d\vartheta} d(p(\vartheta_0 + \vartheta), p(\vartheta_0))$. To expand to the quantum case, one can assume a pair of quantum states ρ and σ , and define $p_x = \text{Tr}[\Pi_x \rho]$ and $q_x = \text{Tr}[\Pi_x \sigma]$ where these are the measurement probabilities corresponding to the positive operator-valued measure (POVM) $\{\Pi_x \geq 0\}$ fulfilling $\sum_x \Pi_x = \mathbb{I}$.

To determine the corresponding quantum statistical distance known as the Hilbert-Schmidt distance⁶¹ represented by $D_{HS}(\rho, \sigma) \equiv \max_{\{\Pi_x\}} d(p, q) = \sqrt{\frac{1}{2} \text{Tr}[(\rho - \sigma)^2]}$, we maximize the classical statistical distance $d(p, q)$ over all possible measurements of POVMs⁶². In the same way, the related quantum statistical speed (QSS) is determined by maximizing the CSS over all possible measurements of POVMs^{57,63}. Hence, assuming the quantum state $\rho(\vartheta)$, one can define the HSS as^{34,57,64}

$$HSS(\vartheta) = \max_{\{\Pi_x\}} s[p(\vartheta)] = \sqrt{\frac{1}{2} \text{Tr} \left[\frac{d\rho(\vartheta)}{d\vartheta} \right]^2}. \quad (3)$$

Bures distance

As mentioned in⁶⁵, another popular witness for quantifying non-Markovianity is the Bures distance. In a similar method for determining the HSS, for an assumed pair of quantum states ρ_{in} and ρ_{fi} , maximizing the classical distance over all possible choices of POVMs, one can define the Bures distance as^{56,57,66}

$$D_{\text{Bures}}(\rho_{in}, \rho_{fi}) = \sqrt{2 - 2\sqrt{f(\rho_{in}, \rho_{fi})}}. \quad (4)$$

where $f(\rho_{in}, \rho_{fi}) = \left(\text{Tr} \left[\sqrt{\sqrt{\rho_{in}} \rho_{fi} \sqrt{\rho_{in}}} \right] \right)^2$ denotes fidelity^{67,68}. It should be noted that we can use the distances to quantify the distinguishability between two quantum states.

Bhattacharyya distance (BD)

We now introduce a new distance that then we can use to identify non-Markovianity for pure quantum states. Considering two arbitrary probability distributions p and q , one can determine the classical Bhattacharyya distance (BD) or geodesic distance as^{55,56,69,70}

$$d_B(p, q) = \cos^{-1} \left(\sum_{i=1}^n \sqrt{p_i q_i} \right), \quad (5)$$

The right-hand side of the equation is called the Bhattacharyya coefficient, and it bears a striking resemblance to the scalar product in quantum mechanics. Its square is referred to as classical fidelity. Moreover, it is clear that the Hellinger distance is a monotone function of the Bhattacharyya distance.

To expand to the quantum case, we assume two states of $|\psi_{in}\rangle$ and $|\psi_{fi}\rangle$. Consider an operator A , and observe that it has $n + 1$ orthogonal eigenstates $|e_i\rangle$ in terms of which we can expand as

$$|\psi_{in}\rangle = \sum_{i=0}^n \sqrt{p_i} e^{i\mu_i} |e_i\rangle, \quad |\psi_{fi}\rangle = \sum_{i=0}^n \sqrt{q_i} e^{i\nu_i} |e_i\rangle, \quad (6)$$

where we suppose p_i and q_i are non-negative real numbers in such a way

$$\sum_{i=0}^n p_i = \sum_{i=0}^n q_i = 1, \quad (7)$$

It means that our states are normalized. Here, μ_i, ν_i represent the phase factors. The probability p_i to obtain a given measurement outcome is obtained through the standard interpretation of quantum mechanics for the i th outcome to happen when the state is $|\psi_{in}\rangle$. According to the mentioned method in⁵⁶ the BD between the given states ψ_1 and ψ_2 , can be determined from the square roots of the probabilities:

$$\cos(d_B) = \sum_{i=0}^n \sqrt{p_i} \sqrt{q_i} = \sum_{i=0}^n |\langle \psi_{in} | i \rangle| |\langle \psi_{fi} | i \rangle|, \quad (8)$$

Concerning the definition of distance between quantum states, we should choose operator A so that d_B is maximized, making the right-hand side as small as possible. However, we have the inequality as follows

$$\sum_{i=0}^n |\langle \psi_{in} | i \rangle| |\langle \psi_{fi} | i \rangle| \geq |\langle \psi_{in} | \psi_{fi} \rangle|, \quad (9)$$

Therefore, the quantum BD which is the distance in the space of pure states can be reduced as

$$D_{\text{Bhatt}}(\psi_{in}, \psi_{fi}) = \cos^{-1} \left(|\langle \psi_{in} | \psi_{fi} \rangle| \right), \quad (10)$$

This distance is sometimes called the quantum angle between two pure states. Furthermore, the threshold of BD is $\pi/2$.

Non-Markovianity measure based on Bhattacharyya distance

It is well known that non-Markovian effects can lead to quicker quantum evolution from an initial state to a subsequent state^{51,71-75}. The Bhattacharyya distance criterion can effectively determine memory effects in system dynamics. Here, we emphasize exploiting the Bhattacharyya distance^{55,56,70} as a valuable witness of the non-Markovian aspect of quantum evolutions, leading to practical benefits in analysis.

Regarding the idea that a nonmonotonic speed (positive acceleration) of quantum dynamics indicates memory effects in the system dynamics, a non-Markovianity witness based on BD can be introduced as

$$\mathcal{I}(t) := \frac{dD_{\text{Bhatt}}(t)}{dt} > 0, \quad (11)$$

If the system interacts with its surrounding environment, i.e. there is a system-environment information exchange, the D_{Bhatt} decreases monotonically, then dynamics is known as Markovian. So, we have for some time intervals $\mathcal{I}(t) < 0$. In contrast, every positive value of $\mathcal{I}(t) > 0$ denotes a witness of non-Markovianity.

According to this witness, similar to what has been done for other measures^{27,34,36,42,76}, a determiner of the degree of non-Markovianity can be defined as

$$\mathcal{N} := \max \int_{\mathcal{I}(t)>0} \mathcal{I}(t)dt, \tag{12}$$

where the maximization is carried out over all possible parameterizations of the initial state. It is essential to note this point that in this article we evaluate the quantity presented in Eq. (12) according to the quantities of Bhattacharyya distance, Bures distance, Hilbert-Schmidt speed, and quantum Fisher information, which expresses the degree of non-Markovian system dynamics.

We aim to only investigate non-Markovian effects using D_{Bhatt} based on the witness, where the actual value is irrelevant and no optimization is performed on the initial state parameters.

The physical models

Two-level atom

We assume the interaction between a single-mode radiation field with frequency ν and a two-level atom (as illustrated in Fig. 1). Suppose $|a\rangle$ and $|b\rangle$ denote the upper and lower level states of the atom, such that they are eigenstates of the unperturbed part of the Hamiltonian \mathcal{H}_0 with the eigenvalues $\hbar\omega_a$ and $\hbar\omega_b$, respectively. We can write the wave function of a two-level atom as the following form

$$|\psi(t)\rangle = C_a(t)|a\rangle + C_b(t)|b\rangle, \tag{13}$$

in which C_a and C_b denote the probability amplitudes of finding the atom in states $|a\rangle$ and $|b\rangle$, respectively. The corresponding Schrödinger equation is defined as

$$i\dot{|\psi(t)\rangle} = -\frac{i}{\hbar}\mathcal{H}|\psi(t)\rangle, \tag{14}$$

with the Hamiltonian of the system

$$\mathcal{H} = \mathcal{H}_0 + \mathcal{H}_1, \tag{15}$$

where \mathcal{H}_0 and \mathcal{H}_1 are the unperturbed and interaction terms of the Hamiltonian, respectively. Utilizing the completeness relation $|a\rangle\langle a| + |b\rangle\langle b| = \mathbf{1}$, one can write the unperturbed part as⁷⁷

$$\mathcal{H}_0 = (|a\rangle\langle a| + |b\rangle\langle b|)\mathcal{H}_0(|a\rangle\langle a| + |b\rangle\langle b|) = \hbar\omega_a|a\rangle\langle a| + \hbar\omega_b|b\rangle\langle b|, \tag{16}$$

such that we used $\mathcal{H}_0|a\rangle = \hbar\omega_a|a\rangle$ and $\mathcal{H}_0|b\rangle = \hbar\omega_b|b\rangle$. Also, another term of the Hamiltonian \mathcal{H}_1 representing the atom's interaction with the radiation field can be expressed as

$$\begin{aligned} \mathcal{H}_1 &= -exE(t) \\ &= -e(|a\rangle\langle a| + |b\rangle\langle b|)x(|a\rangle\langle a| + |b\rangle\langle b|)E(t) \\ &= -(\wp_{ab}|a\rangle\langle b| + \wp_{ba}|b\rangle\langle a|)E(t), \end{aligned} \tag{17}$$

where $\wp_{ab} = \wp_{ba}^* = e\langle a|x|b\rangle$ represents the matrix element of the electric dipole moment and $E(t)$ denotes the field at the atom. We suppose the electric field is linearly polarized along the x -axis and in the dipole approximation such that $E(t) = E \cos(\nu t)$, where E depicts the amplitude and $\nu = ck$ represents the field frequency.

The motion equations of the system can be written as

$$\begin{aligned} \dot{C}_a &= -i\omega_a C_a + i\Omega_R e^{-i\phi} \cos(\nu t) C_b, \\ \dot{C}_b &= -i\omega_b C_b + i\Omega_R e^{i\phi} \cos(\nu t) C_a, \end{aligned} \tag{18}$$

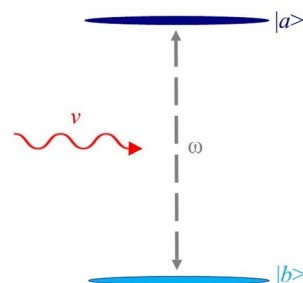


Figure 1. Schematic of the interaction of a two-level atom with a single-mode field.

where $\Omega_R = \frac{|\rho_{ba}|E}{\hbar}$ is the Rabi frequency, and ϕ represents the phase of the dipole matrix element $\rho_{ba} = |\rho_{ba}| \exp(i\phi)$.

To solve for C_a and C_b , we begin by considering the motion equations for the slowly varying amplitudes:

$$\begin{aligned} c_a &= C_a e^{i\omega_a t}, \\ c_b &= C_b e^{i\omega_b t}. \end{aligned} \tag{19}$$

It next obeys from Eq. (18) that

$$\begin{aligned} \dot{c}_a &= i \frac{\Omega_R}{2} e^{-i\phi} c_b e^{i(\omega-\nu)t}, \\ \dot{c}_b &= i \frac{\Omega_R}{2} e^{i\phi} c_a e^{-i(\omega-\nu)t}, \end{aligned} \tag{20}$$

where $\omega = \omega_a - \omega_b$ denotes the atomic transition frequency. After some straight calculations and ignoring the terms $\exp[\pm i(\omega + \nu)t]$, the solutions for ca and cb can be obtained as

$$\begin{aligned} c_a(t) &= (a_1 e^{i\Omega t/2} + a_2 e^{-i\Omega t/2}) e^{i\Delta t/2}, \\ c_b(t) &= (b_1 e^{i\Omega t/2} + b_2 e^{-i\Omega t/2}) e^{-i\Delta t/2}, \end{aligned} \tag{21}$$

where we have $\Delta = \omega - \nu, \Omega = \sqrt{\Omega_R^2 + (\omega - \nu)^2}$, and a_1, a_2, b_1, b_2 are constants of integration which are determined from the initial conditions:

$$\begin{aligned} a_1 &= \frac{1}{2\Omega} [(\Omega - \Delta)c_a(0) + \Omega_R e^{-i\phi} c_b(0)], \\ a_2 &= \frac{1}{2\Omega} [(\Omega + \Delta)c_a(0) - \Omega_R e^{-i\phi} c_b(0)], \\ b_1 &= \frac{1}{2\Omega} [(\Omega + \Delta)c_b(0) + \Omega_R e^{i\phi} c_a(0)], \\ b_2 &= \frac{1}{2\Omega} [(\Omega - \Delta)c_b(0) - \Omega_R e^{i\phi} c_a(0)]. \end{aligned} \tag{22}$$

Finally, we can write as follows

$$\begin{aligned} c_a(t) &= \left\{ c_a(0) \left[\cos\left(\frac{\Omega t}{2}\right) - \frac{i\Delta}{\Omega} \sin\left(\frac{\Omega t}{2}\right) \right] + i \frac{\Omega_R}{\Omega} e^{-i\phi} c_b(0) \sin\left(\frac{\Omega t}{2}\right) \right\} e^{i\Delta t/2}, \\ c_b(t) &= \left\{ c_b(0) \left[\cos\left(\frac{\Omega t}{2}\right) + \frac{i\Delta}{\Omega} \sin\left(\frac{\Omega t}{2}\right) \right] + i \frac{\Omega_R}{\Omega} e^{i\phi} c_a(0) \sin\left(\frac{\Omega t}{2}\right) \right\} e^{-i\Delta t/2}. \end{aligned} \tag{23}$$

such that $|c_a(t)|^2 + |c_b(t)|^2 = 1$. If we assume that the atom is initially in the state $|a\rangle$ the we have $c_a(0) = 1$ and $c_b(0) = 0$.

Three-level atom

We suppose a three-level atom in the Λ configuration interacting with two electromagnetic fields with frequencies ν_1 and ν_2 . As shown in Fig. 2, two lower levels $|b\rangle$ and $|c\rangle$ are commonly coupled to an upper level $|a\rangle$.

The system's Hamiltonian in the rotating-wave approximation is described by Eq. (15), in which

$$\mathcal{H}_0 = \hbar\omega_a |a\rangle\langle a| + \hbar\omega_b |b\rangle\langle b| + \hbar\omega_c |c\rangle\langle c| \tag{24}$$

represents the unperturbed Hamiltonian having eigenvalues $\{\hbar\omega_a, \hbar\omega_b, \hbar\omega_c\}$, and

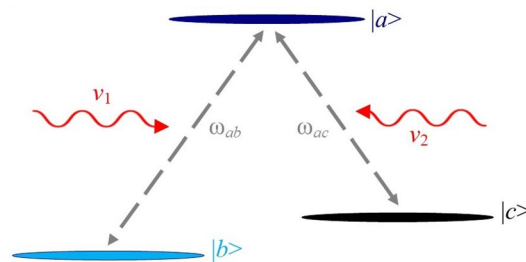


Figure 2. Schematic of a three-level atom in the Λ configuration which are driven by two fields of frequencies ν_1 and ν_2 .

$$\mathcal{H}_1 = -\frac{\hbar}{2}(\Omega_{R1}e^{-i\phi_1}e^{-i\nu_1 t}|a\rangle\langle b| + \Omega_{R2}e^{-i\phi_2}e^{-i\nu_2 t}|a\rangle\langle c|) + H.C. \tag{25}$$

denotes the Hamiltonian that describes the interaction between the atom and fields. Furthermore, $\Omega_{R1}e^{-i\phi_1}$ and $\Omega_{R2}e^{-i\phi_2}$ are the complex Rabi frequencies corresponding to the coupling of the field modes with the frequencies ν_1 and ν_2 to the atomic transitions $|a\rangle \rightarrow |b\rangle$ and $|a\rangle \rightarrow |c\rangle$, respectively. Moreover, ϕ_1 and ϕ_2 are phases of the fields with Rabi frequencies. We only assume $|a\rangle \rightarrow |b\rangle$ and $|a\rangle \rightarrow |c\rangle$ transitions are permissible dipole.

If the system is prepared in the initial atomic state

$$|\psi_{in}\rangle = \cos\left(\frac{\theta}{2}\right)|b\rangle + e^{-i\psi}\sin\left(\frac{\theta}{2}\right)|c\rangle, \tag{26}$$

that is a superposition of the two lower levels $\{|b\rangle, |c\rangle\}$, and consider the fields are in the resonant state with the transitions of $|a\rangle \rightarrow |b\rangle$ and $|a\rangle \rightarrow |c\rangle$, i.e. $\omega_{ab} = \nu_1$ and $\omega_{ac} = \nu_2$, then one can write the evolved state of the system as⁷⁷

$$|\psi_{fi}(t)\rangle = c_a(t)e^{-i\omega_a t}|a\rangle + c_b(t)e^{-i\omega_b t}|b\rangle + c_c(t)e^{-i\omega_c t}|c\rangle, \tag{27}$$

such that using the probability amplitude method, the probability amplitudes of finding the atom in states $|a\rangle$, $|b\rangle$, and $|c\rangle$ are given by

$$\begin{aligned} c_a &= \frac{i \sin(\Omega t/2)}{2} \left[\Omega_{R1}e^{-i\phi_1} \cos\left(\frac{\theta}{2}\right) + \Omega_{R2}e^{-i(\phi_2+\psi)} \sin\left(\frac{\theta}{2}\right) \right], \\ c_b &= \frac{1}{\Omega^2} \left\{ \left[\Omega_{R2}^2 + \Omega_{R1}^2 \cos\left(\frac{\Omega t}{2}\right) \right] \cos\left(\frac{\theta}{2}\right) - 2\Omega_{R1}\Omega_{R2}e^{i(\phi_1-\phi_2-\psi)} \sin^2\left(\frac{\Omega t}{4}\right) \sin\left(\frac{\theta}{2}\right) \right\}, \\ c_c &= \frac{1}{\Omega^2} \left\{ -2\Omega_{R1}\Omega_{R2}e^{-i(\phi_1-\phi_2)} \sin^2\left(\frac{\Omega t}{4}\right) \cos\left(\frac{\theta}{2}\right) + \left[\Omega_{R1}^2 + \Omega_{R2}^2 \cos\left(\frac{\Omega t}{2}\right) \right] e^{-i\psi} \sin\left(\frac{\theta}{2}\right) \right\}. \end{aligned} \tag{28}$$

in which $\Omega = \sqrt{\Omega_{R1}^2 + \Omega_{R2}^2}$. where θ and ψ are the amplitude and phase of the initial state. Besides, ϕ_1 and ϕ_2 are the initial phases of the fields.

Throughout this paper, we consider $\hbar = 1$ and all parameters are nondimensionalized to plot the figures as mentioned in Refs.^{78,79}.

Two effective two-level atoms

The system contains two effective two-level atoms that are considered as two similar qubits *A* and *B* interacting locally with two independent environments R_1 and R_2 , respectively, such that are modeled as bosonic reservoirs at zero temperature. The schematic of two two-level atoms at this configuration is illustrated in Fig. 3. We consider the qubit system in each environment interacts with the environment's field through degenerate two-photon transitions in the presence of the Stark shift. The transition frequencies of the environment modes ω_{kj} , ($j = 1, 2$) corresponding to R_1 and R_2 . Besides ω_0 represents the transition frequency of the two qubits. In the rotating wave approximation, the effective Hamiltonian for the current model is written by ($\hbar = 1$)^{80,81}:

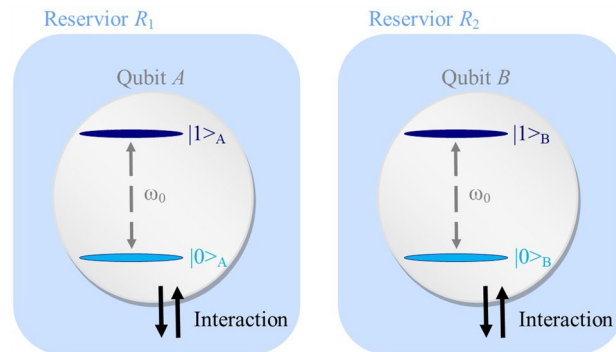


Figure 3. Schematic of the configuration of two effective two-level atoms (qubits *A*, and *B*) interacting independently with their reservoirs R_1 , and R_2 . There is no interaction between the two subsystems.

$$\begin{aligned} \hat{H}_{\text{eff}} = & \omega_0(\hat{\sigma}_+^A \hat{\sigma}_-^A + \hat{\sigma}_+^B \hat{\sigma}_-^B) + \sum_{k_1} \omega_{k_1} \hat{a}_{k_1}^\dagger \hat{a}_{k_1} + \sum_{k_2} \omega_{k_2} \hat{a}_{k_2}^\dagger \hat{a}_{k_2} \\ & + \sum_{k_1} g_{k_1} (\hat{a}_{k_1}^{\dagger 2} \hat{\sigma}_-^A + \hat{a}_{k_1}^2 \hat{\sigma}_+^A) + \sum_{k_1} \hat{a}_{k_1}^\dagger \hat{a}_{k_1} (\beta_{k_1} \hat{\sigma}_-^A \hat{\sigma}_+^A + \eta_{k_1} \hat{\sigma}_+^A \hat{\sigma}_-^A) \\ & + \sum_{k_2} g_{k_2} (\hat{a}_{k_2}^{\dagger 2} \hat{\sigma}_-^B + \hat{a}_{k_2}^2 \hat{\sigma}_+^B) + \sum_{k_2} \hat{a}_{k_2}^\dagger \hat{a}_{k_2} (\beta_{k_2} \hat{\sigma}_-^B \hat{\sigma}_+^B + \eta_{k_2} \hat{\sigma}_+^B \hat{\sigma}_-^B). \end{aligned} \tag{29}$$

where $\hat{\sigma}_\pm^{A,B}$ denote atomic raising and lowering operators of the qubits A, and B. Besides, $\hat{a}_{k_j}^\dagger$ and \hat{a}_{k_j} represent the creation and annihilation operators of the k th mode of the j th environment ($j = 1, 2$). Moreover, g_{k_1} and g_{k_2} determine the effective two-photon strength of the qubit environment corresponding to the modes k_1 and k_2 , respectively. Furthermore, β_{k_j} and η_{k_j} are the effective Stark shift coefficients⁸². Rewriting the previous Hamiltonian in the interaction picture is convenient:

$$\begin{aligned} \hat{H}_{\text{int}} = & \sum_{k_1} g_{k_1} (\hat{a}_{k_1}^{\dagger 2} \hat{\sigma}_-^A e^{-i(\omega_0 - 2\omega_{k_1})t} + \hat{a}_{k_1}^2 \hat{\sigma}_+^A e^{i(\omega_0 - 2\omega_{k_1})t}) \\ & + \sum_{k_1} \hat{a}_{k_1}^\dagger \hat{a}_{k_1} (\beta_{k_1} \hat{\sigma}_-^A \hat{\sigma}_+^A + \eta_{k_1} \hat{\sigma}_+^A \hat{\sigma}_-^A) \\ & + \sum_{k_2} g_{k_2} (\hat{a}_{k_2}^{\dagger 2} \hat{\sigma}_-^B e^{-i(\omega_0 - 2\omega_{k_2})t} + \hat{a}_{k_2}^2 \hat{\sigma}_+^B e^{i(\omega_0 - 2\omega_{k_2})t}) \\ & + \sum_{k_2} \hat{a}_{k_2}^\dagger \hat{a}_{k_2} (\beta_{k_2} \hat{\sigma}_-^B \hat{\sigma}_+^B + \eta_{k_2} \hat{\sigma}_+^B \hat{\sigma}_-^B). \end{aligned} \tag{30}$$

We assume the system is in the initial state as:

$$|\phi(0)\rangle = (\chi|0\rangle_A|1\rangle_B + \sqrt{1 - \chi^2}|1\rangle_A|0\rangle_B) \otimes |0_{k_1}\rangle_{R_1} |0_{k_2}\rangle_{R_2}, \tag{31}$$

in which $\chi \in [0, 1]$, where $|0_{k_j}\rangle_{R_j}$ represents the vacuum state of the j th environment, and $|0\rangle_j, |1\rangle_j$ ($j = A, B$) denote the ground and excited states of the two-level atoms. The number of excitations in the total system is preserved, thus the time evolution of the total system can be obtained by

$$\begin{aligned} |\phi(t)\rangle = & (c_1(t)|1\rangle_A|0\rangle_B + c_2(t)|0\rangle_A|1\rangle_B) |0_{k_1}\rangle_{R_1} |0_{k_2}\rangle_{R_2} \\ & + \sum_{k_1} c_{k_1}(t) |0\rangle_A|0\rangle_B |2_{k_1}\rangle_{R_1} |0_{k_2}\rangle_{R_2} \\ & + \sum_{k_2} c_{k_2}(t) |0\rangle_A|0\rangle_B |0_{k_1}\rangle_{R_1} |2_{k_2}\rangle_{R_2}, \end{aligned} \tag{32}$$

where $|2_{k_j}\rangle_{R_j}$ denotes excitations of two photons in the mode k for the j th environment. It's worth noting that the two-photon process is considered, and then the j th environment has only two states $|0_{k_j}\rangle$ and $|2_{k_j}\rangle$. Using the probability amplitude method, Laplace technique, and the similar method given by Refs.^{80,81}, the probability amplitude coefficients can be written as:

$$c_1(t) = \chi \xi(t), \quad c_2(t) = \sqrt{1 - \chi^2} \xi(t), \tag{33}$$

with

$$\xi(t) = e^{-\frac{(\lambda + 2i\beta)t}{2}} \left[\cosh\left(\frac{\varrho t}{2}\right) + \frac{\lambda + 2i\beta}{\varrho} \sinh\left(\frac{\varrho t}{2}\right) \right],$$

and

$$\varrho = \sqrt{-4\gamma_0\lambda + (\lambda + 2i\beta)^2}.$$

We are facing two regimes, i.e. weak ($\gamma_0 < \lambda/2$) and strong ($\gamma_0 > \lambda/2$) coupling regimes⁸³. In the weak coupling regime, the relaxation time is more than the reservoir correlation time, where the behavior of the qubit-reservoir system is Markovian and a decay process arises in the time. In contrast, when the reservoir correlation time exceeds the relaxation time, non-Markovian dynamics emerge, leading to a strong coupling regime. The entanglement revival, accompanied by oscillations due to the reservoir memory effect, becomes observable.

Consider the Hermitian matrix $\hat{H} = \hat{\rho} \hat{\rho}_s$, in which $\hat{\rho}$ indicates the reduced density matrix of the pair of qubits A, B and $\hat{\rho}_s = (\hat{\sigma}_y^A \otimes \hat{\sigma}_y^B) \rho^* (\hat{\sigma}_y^A \otimes \hat{\sigma}_y^B)$, with ρ^* as the complex conjugate of $\hat{\rho}$ and $\hat{\sigma}_y^A, \hat{\sigma}_y^B$ as the usual Pauli matrices for the qubits. Assuming the atomic basis $\{|1\rangle_A|1\rangle_B, |1\rangle_A|0\rangle_B, |0\rangle_A|1\rangle_B, |0\rangle_A|0\rangle_B\}$, one can calculate the time-dependence of the reduced density matrix as^{80,81}:

$$\rho(t) = \begin{pmatrix} 0 & 0 & 0 & 0 \\ 0 & |c_1(t)|^2 & c_1(t)c_2^*(t) & 0 \\ 0 & c_1^*(t)c_2(t) & |c_2(t)|^2 & 0 \\ 0 & 0 & 0 & 1 - |c_1(t)|^2 - |c_2(t)|^2 \end{pmatrix}. \tag{34}$$

Discussion and results

Here we display that memory effects can be extracted by faithful witnesses of non-Markovianity based on the Bhattacharyya distance. As illustrated in Fig. 4, using straightforward expressions in Appendix A, we compare the qualitative behaviors of the Bhattacharyya distance (D_{Bhatt}), the Bures distance (D_{Bures}), Hilbert-Schmidt speed (HSS_ϕ), and quantum Fisher information (\mathcal{F}_ϕ) with respect to the phase of the dipole matrix element for a two-level atom scenario. We can clearly see that the qualitative behavior of D_{Bhatt} is completely similar to other quantities so that the maximum and minimum points of the curves coincide with each other. As mentioned in Refs.^{32,34}, a flow of QFI and HSS, i.e., $\frac{d(\mathcal{F}_\phi)}{dt} > 0$ and $\frac{d(HSS_\phi)}{dt} > 0$, in which the QFI and HSS have been calculated with respect to the phase ϕ , can detect the non-Markovianity effects. Hence the positive changing rate of the Bhattacharyya distance, i.e., $\frac{d(D_{Bhatt})}{dt} > 0$, can also detect the memory effects. This non-Markovianity witness is in total agreement with other witnesses based on Bures distance, QFI, and HSS thus identifying the information backflows.

Next, we expand the efficiency of our witness to the system with higher dimensions. In Fig. 5, the qualitative behaviors of the Bhattacharyya distance (D_{Bhatt}) and the Bures distance (D_{Bures}) for the three-level atom scenario are demonstrated. Here we see that the general agreement of the similar behaviors of the two quantities D_{Bhatt} and D_{Bures} for a three-level atom system still stands.

Furthermore, we show the comparison between time evolutions of the D_{Bhatt} , D_{Bures} , $HSS_{\phi 1}$, and $\mathcal{F}_{\phi 1}$ with respect to the phase of the fields for the three-level atom scenario in Fig. 6. The result that can be obtained from this figure is that the qualitative behaviors of the D_{Bhatt} , D_{Bures} , $HSS_{\phi 1}$, and $\mathcal{F}_{\phi 1}$ in high dimensions systems are exactly similar. These results are also valid for other different values of the system parameters. In addition, these results can be extended to other models.

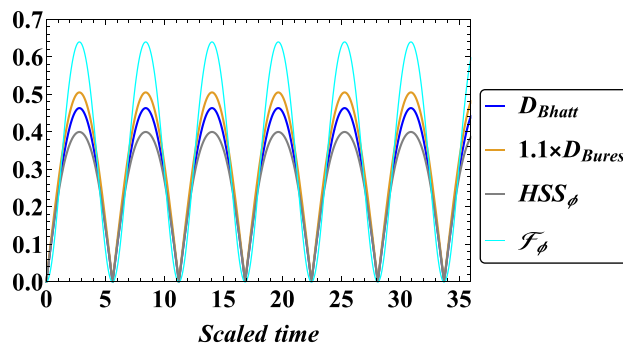


Figure 4. Comparison between the dynamics of the Bhattacharyya distance (D_{Bhatt}), Bures distance (D_{Bures}), Hilbert-Schmidt speed (HSS_ϕ), and quantum Fisher information (\mathcal{F}_ϕ) with respect to the phase of the dipole matrix element for the two-level atom scenario when $\Omega_R = 0.5$ and $\Delta = 1$.

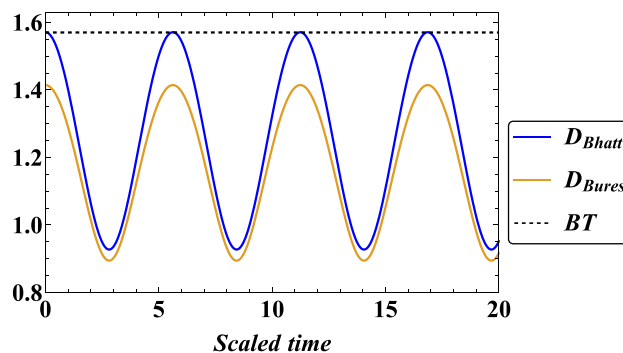


Figure 5. Comparison between the temporal variations of the Bhattacharyya distance (D_{Bhatt}) and Bures distance (D_{Bures}) for the three-level atom scenario when $\Omega_{R1} = 1, \Omega_{R2} = 2, \omega_a = \omega_b = \omega_c = 1, \varphi = 2\pi, \phi_1 = \phi_2 = \psi = \pi$ and $\theta = \pi/2$. Here, $BT = 1.57$ represents the Bhattacharyya distance threshold.

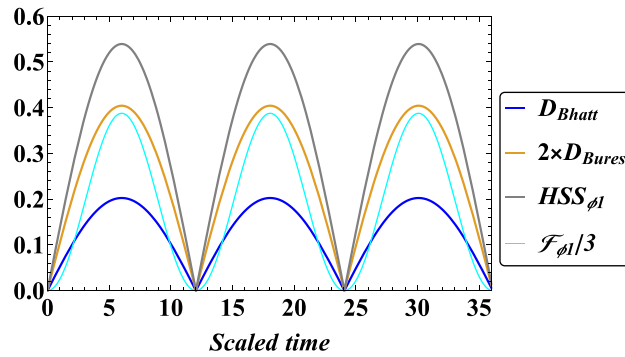


Figure 6. Comparison between the qualitative behaviors of the Bhattacharyya distance (D_{Bhatt}), the Bures distance (D_{Bures}), Hilbert-Schmidt speed ($HSS_{\phi 1}$), and quantum Fisher information ($\mathcal{F}_{\phi 1}$) with respect to the phase of the fields in terms of scaled time for the three-level atom scenario when $\Omega_{R1} = 0.3, \Omega_{R2} = 1, \omega_a = 0.9, \omega_b = \omega_c = 1, \varphi = \phi_1 = \phi_2 = \psi = \pi$ and $\theta = \pi/4$.

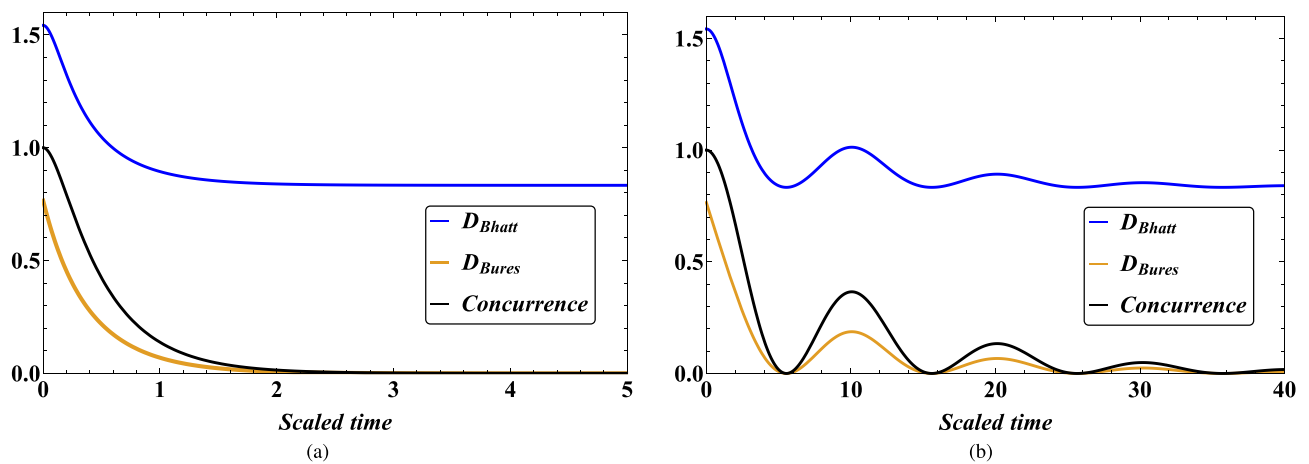


Figure 7. Comparison between the temporal variations of the Bhattacharyya distance (D_{Bhatt}), the Bures distance (D_{Bures}), and concurrence for two effective two-level atoms system for (a) Markovian reservoir when $\lambda = 10, \beta = 0, \gamma_0 = 1, \chi = \frac{1}{\sqrt{2}}$, (b) Non-Markovian reservoir $\lambda = 0.1, \beta = 0, \gamma_0 = 1, \chi = \frac{1}{\sqrt{2}}$.

In Fig. 7, we investigate the qualitative behaviors of the D_{Bhatt} , D_{Bures} , and concurrence for the two effective two-level atoms system. The concurrence measure⁸⁴ is employed as an entanglement criterion defined as $Concurrence = \max\{0, \sqrt{\lambda_1} - \sqrt{\lambda_2} - \sqrt{\lambda_3} - \sqrt{\lambda_4}\}$ where λ_i ($i = 1, \dots, 4$) represents the eigenvalues of the evolved density matrix Eq. (34). In Fig. 7, we observe that the qualitative behaviors of the D_{Bhatt} , D_{Bures} , and concurrence are similar such that the minimum and maximum points of the behaviors coincide. This allows D_{Bhatt} to examine the entanglement dynamics of the system along with non-Markovian effects, making it highly beneficial in quantum computing. In a weak coupling regime ($\gamma_0 < \lambda/2$), Fig. 7a, the monotonicity decrease of D_{Bhatt} , D_{Bures} , and concurrence is obvious. Here, the relaxation time is more than the reservoir correlation time, where the behavior of the qubit-reservoir system is Markovian and a decay process arises in the time. While in a strong coupling regime ($\gamma_0 > \lambda/2$), Fig. 7b, the D_{Bhatt} , D_{Bures} , and concurrence revivals, accompanied by oscillations due to the reservoir memory effect, becomes observable. It means that the reservoir correlation time exceeds the relaxation time, leading to non-Markovian dynamics emerging.

Therefore, it can be easily stated that Bhattacharyya quantum distance can well detect the non-Markovian dynamics caused by quantum memory effects. As stated in Appendix A, it can be seen that this distance does not require heavy calculations in pure states, and only by having the initial and final states of the system, the effects of quantum memory can be detected. This point is important in high-dimension systems because of difficult calculations.

Conclusion

In this article, we have determined a relation between the positive changing rate of the Bhattacharyya distance (BD), a particular type of quantum statistical distance, and the non-Markovian dynamics of open quantum systems. The concept behind this suggestion is based on the idea that the nonmonotonic speed (positive acceleration) of quantum evolutions indicates memory effects in the dynamics of the system interacting with its

environment. Through the introduction of a BD-based quantifier, a quantitative witness of memory effects in system dynamics can be defined.

In an extensive case study analysis, we have demonstrated that the suggested witness is as useful as the well-known witnesses of quantum Fisher information (QFI), Bures distance, and Hilbert-Schmidt speed (HSS) in identifying non-Markovianity. The models analyzed in our paper include various paradigmatic open quantum systems (two and three-level atoms interacting single and two-mode fields, respectively, and two effective two-level atoms interacting locally with two independent environments) and provide proof of the sensitivity of our BD witness to system-environment information backflows. We note that non-Markovianity witness of the BD does not require the computation of the density matrix, but only determines it from the initial and final states of the system thereby leading to the improvement of the quantum metrology. One crucial finding in this article is that the BD measure can be used as a measure of entanglement like the Bures distance. Therefore, a quantifier with this characteristic would be highly sought after.

This article motivates further analysis of the role of non-Markovian effects in different open quantum systems and their relationship to quantum statistical distances.

Data availability

All data generated or analyzed during this study are included in this paper.

Appendix A: Straightforward expressions

Two-level atom

By inserting Eqs. (13) and (23) in Eq. (2) and with using $(\rho_{fi} = |\psi_{fi}\rangle\langle\psi_{fi}|)$, one can obtain the straightforward expression of quantum estimation with respect to phase ϕ with employing QFI in two-level atom scenario as

$$\mathcal{F}_\phi = \frac{1}{(\Delta^2 + \Omega_R^2)^2} 2\Omega_R^2 \sin^2\left(\frac{1}{2}t\sqrt{\Delta^2 + \Omega_R^2}\right) \times \left(2\Delta^2 + \Omega_R^2 \cos\left(t\sqrt{\Delta^2 + \Omega_R^2}\right) + \Omega_R^2\right), \quad (37)$$

Moreover, using the same method for Eq. (35) and utilizing Eq. (3), one can calculate the straightforward expression for quantum estimation with respect to phase ϕ with employing HSS in two-level atom scenario as

$$HSS_\phi = \frac{\Omega_R \sqrt{\frac{\sin^2\left(\frac{1}{2}t\sqrt{\Delta^2 + \Omega_R^2}\right) \left(2\Delta^2 + \Omega_R^2 \cos\left(t\sqrt{\Delta^2 + \Omega_R^2}\right) + \Omega_R^2\right)}{(\Delta^2 + \Omega_R^2)^2}}}{\sqrt{2}}, \quad (38)$$

Furthermore, using Eq. (4), we have the straightforward expression for Bures distance between initial density matrix ρ_{in} and evolved density matrix ρ_{fi} as follows

$$D_{Bures} = \sqrt{2 - \sqrt{2} \sqrt{\frac{2\Delta^2 + \Omega_R^2 \cos\left(t\sqrt{\Delta^2 + \Omega_R^2}\right) + \Omega_R^2}{\Delta^2 + \Omega_R^2}}}, \quad (39)$$

At final, utilizing Eq. (10) and initial state $|\psi_{in}\rangle$ and evolved state $|\psi_{fi}\rangle$, one can calculate the straightforward expression for BD by

$$D_{Bhatt} = \cos^{-1}\left(\frac{\sqrt{\frac{2\Delta^2 + \Omega_R^2 \cos\left(t\sqrt{\Delta^2 + \Omega_R^2}\right) + \Omega_R^2}{\Delta^2 + \Omega_R^2}}}{\sqrt{2}}\right). \quad (40)$$

It should be noted that due to the cumbersome form for the expressions in the three-level atom scenario, we refrain from reporting them here.

Received: 8 May 2024; Accepted: 31 July 2024

Published online: 06 August 2024

References

1. Breuer, H.-P. & Petruccione, F. *The Theory of Open Quantum Systems* (Oxford University Press, 2002).
2. Rivas, A. & Huelga, S. F. *Open Quantum Systems* Vol. 10 (Springer, 2012).
3. Cai, X. *et al.* Quantum dynamical speedup in a nonequilibrium environment. *Phys. Rev. A* **95**, 052104 (2017).
4. Cai, X. & Zheng, Y. Non-Markovian decoherence dynamics in nonequilibrium environments. *J. Chem. Phys.* **149**, 85 (2018).
5. Cai, X. Quantum dephasing induced by non-Markovian random telegraph noise. *Sci. Rep.* **10**, 88 (2020).
6. Czerwinski, A. Quantum communication with polarization-encoded qubits under majorization monotone dynamics. *Mathematics* **10**, 3932 (2022).
7. De Vega, I. & Alonso, D. Dynamics of non-Markovian open quantum systems. *Rev. Mod. Phys.* **89**, 015001 (2017).
8. Breuer, H.-P., Laine, E.-M., Piilo, J. & Vacchini, B. Colloquium: Non-Markovian dynamics in open quantum systems. *Rev. Mod. Phys.* **88**, 021002 (2016).

9. Rivas, Á., Huelga, S. F. & Plenio, M. B. Quantum non-Markovianity: Characterization, quantification and detection. *Rep. Prog. Phys.* **77**, 094001 (2014).
10. Franco, R. L., Bellomo, B., Maniscalco, S. & Compagno, G. Dynamics of quantum correlations in two-qubit systems within non-Markovian environments. *Int. J. Mod. Phys. B* **27**, 1345053 (2013).
11. Mortezaipour, A., Naeimi, G. & Franco, R. L. Coherence and entanglement dynamics of vibrating qubits. *Opt. Commun.* **424**, 26 (2018).
12. Caruso, F., Giovannetti, V., Lupo, C. & Mancini, S. Quantum channels and memory effects. *Rev. Mod. Phys.* **86**, 1203 (2014).
13. Gholipour, H., Mortezaipour, A., Nosrati, F. & Franco, R. L. Quantumness and memory of one qubit in a dissipative cavity under classical control. *Ann. Phys.* **414**, 168073 (2020).
14. D'Arrigo, A., Franco, R. L., Benenti, G., Paladino, E. & Falci, G. Recovering entanglement by local operations. *Ann. Phys.* **350**, 211 (2014).
15. Xu, J.-S. *et al.* Experimental recovery of quantum correlations in absence of system-environment back-action. *Nat. Commun.* **4**, 2851 (2013).
16. Smirne, A., Mazzola, L., Paternostro, M. & Vacchini, B. Interaction-induced correlations and non-Markovianity of quantum dynamics. *Phys. Rev. A* **87**, 052129 (2013).
17. Mazzola, L., Rodriguez-Rosario, C. A., Modi, K. & Paternostro, M. Dynamical role of system-environment correlations in non-Markovian dynamics. *Phys. Rev. A* **86**, 010102 (2012).
18. Bernardes, N. K. *et al.* Experimental observation of weak non-Markovianity. *Sci. Rep.* **5**, 17520 (2015).
19. Bernardes, N. K. *et al.* High resolution non-Markovianity in NMR. *Sci. Rep.* **6**, 33945 (2016).
20. Liu, B.-H. *et al.* Experimental control of the transition from Markovian to non-Markovian dynamics of open quantum systems. *Nat. Phys.* **7**, 931 (2011).
21. Laine, E.-M., Breuer, H.-P. & Piilo, J. Nonlocal memory effects allow perfect teleportation with mixed states. *Sci. Rep.* **4**, 4620 (2014).
22. Bylicka, B., Tukiainen, M., Chruściński, D., Piilo, J. & Maniscalco, S. Thermodynamic power of non-Markovianity. *Sci. Rep.* **6**, 27989 (2016).
23. Xiang, G.-Y. *et al.* Entanglement distribution in optical fibers assisted by nonlocal memory effects. *Europhys. Lett.* **107**, 54006 (2014).
24. Mirkin, N., Poggi, P. & Wisniacki, D. Information backflow as a resource for entanglement. *Phys. Rev. A* **99**, 062327 (2019).
25. Mirkin, N., Poggi, P. & Wisniacki, D. Entangling protocols due to non-Markovian dynamics. *Phys. Rev. A* **99**, 020301 (2019).
26. Thomas, G., Siddharth, N., Banerjee, S. & Ghosh, S. Thermodynamics of non-Markovian reservoirs and heat engines. *Phys. Rev. E* **97**, 062108 (2018).
27. Breuer, H.-P., Laine, E.-M. & Piilo, J. Measure for the degree of non-Markovian behavior of quantum processes in open systems. *Phys. Rev. Lett.* **103**, 210401 (2009).
28. Chen, H. *et al.* Quantum state tomography in nonequilibrium environments. *Photonics* **10**, 134 (2023).
29. Teittinen, J., Lyyra, H., Sokolov, B. & Maniscalco, S. Revealing memory effects in phase-covariant quantum master equations. *New J. Phys.* **20**, 073012 (2018).
30. Naikoo, J., Dutta, S. & Banerjee, S. Facets of quantum information under non-Markovian evolution. *Phys. Rev. A* **99**, 042128 (2019).
31. Luo, S., Fu, S. & Song, H. Quantifying non-Markovianity via correlations. *Phys. Rev. A* **86**, 044101 (2012).
32. Lu, X.-M., Wang, X. & Sun, C. Quantum Fisher information flow and non-Markovian processes of open systems. *Phys. Rev. A* **82**, 042103 (2010).
33. Rangani Jahromi, H. Relation between quantum probe and entanglement in n-qubit systems within Markovian and non-Markovian environments. *J. Mod. Opt.* **64**, 1377 (2017).
34. Jahromi, H. R., Mahdaviipour, K., Shadfar, M. K. & Franco, R. L. Witnessing non-Markovian effects of quantum processes through Hilbert-Schmidt speed. *Phys. Rev. A* **102**, 022221 (2020).
35. Rivas, Á., Huelga, S. F. & Plenio, M. B. Entanglement and non-Markovianity of quantum evolutions. *Phys. Rev. Lett.* **105**, 050403 (2010).
36. Laine, E.-M., Piilo, J. & Breuer, H.-P. Measure for the non-Markovianity of quantum processes. *Phys. Rev. A* **81**, 062115 (2010).
37. Hall, M. J., Cresser, J. D., Li, L. & Andersson, E. Canonical form of master equations and characterization of non-Markovianity. *Phys. Rev. A* **89**, 042120 (2014).
38. He, Z., Yao, C., Wang, Q. & Zou, J. Measuring non-Markovianity based on local quantum uncertainty. *Phys. Rev. A* **90**, 042101 (2014).
39. Chanda, T. & Bhattacharya, S. Delineating incoherent non-Markovian dynamics using quantum coherence. *Ann. Phys.* **366**, 1 (2016).
40. He, Z., Zeng, H.-S., Li, Y., Wang, Q. & Yao, C. Non-Markovianity measure based on the relative entropy of coherence in an extended space. *Phys. Rev. A* **96**, 022106 (2017).
41. Rajagopal, A., Devi, A. U. & Rendell, R. Kraus representation of quantum evolution and fidelity as manifestations of Markovian and non-Markovian forms. *Phys. Rev. A* **82**, 042107 (2010).
42. Hesabi, S. & Afshar, D. Non-Markovianity measure of Gaussian channels based on fidelity of teleportation. *Phys. Lett. A* **410**, 127482 (2021).
43. Bylicka, B., Chruściński, D. & Maniscalco, S. Non-Markovianity and reservoir memory of quantum channels: A quantum information theory perspective. *Sci. Rep.* **4**, 5720 (2014).
44. Dhar, H. S., Bera, M. N. & Adesso, G. Characterizing non-Markovianity via quantum interferometric power. *Phys. Rev. A* **91**, 032115 (2015).
45. Girolami, D. *et al.* Quantum discord determines the interferometric power of quantum states. *Phys. Rev. Lett.* **112**, 210401 (2014).
46. Fanchini, F. F., Pinto, D. D. O. S. & Adesso, G. *Lectures on General Quantum Correlations and Their Applications* (Springer, 2017).
47. Zheng, X., Ma, S.-Q. & Zhang, G.-F. Annalen der Physik Detecting Non-Markovianity via linear entropy of Choi state. *Ann. Phys.* **532**, 1900320 (2020).
48. Lorenzo, S., Plastina, F. & Paternostro, M. Geometrical characterization of non-Markovianity. *Phys. Rev. A* **88**, 020102 (2013).
49. De Santis, D., Johansson, M., Bylicka, B., Bernardes, N. K. & Acín, A. Correlation measure detecting almost all non-Markovian evolutions. *Phys. Rev. A* **99**, 012303 (2019).
50. Zhang, W.-M., Lo, P.-Y., Xiong, H.-N., Tu, M.W.-Y. & Nori, F. General non-Markovian dynamics of open quantum systems. *Phys. Rev. Lett.* **109**, 170402 (2012).
51. Deffner, S. & Lutz, E. Quantum speed limit for non-Markovian dynamics. *Phys. Rev. Lett.* **111**, 010402 (2013).
52. Xu, Z.-Y., Luo, S., Yang, W., Liu, C. & Zhu, S. Quantum speedup in a memory environment. *Phys. Rev. A* **89**, 012307 (2014).
53. Xu, K., Zhang, Y.-J., Xia, Y.-J., Wang, Z. & Fan, H. Hierarchical-environment-assisted non-Markovian speedup dynamics control. *Phys. Rev. A* **98**, 022114 (2018).
54. Strasberg, P. & Esposito, M. Non-Markovianity and negative entropy production rates. *Phys. Rev. E* **99**, 012120 (2019).
55. Bhattacharyya, A. On a measure of divergence between two multinomial populations. *Sankhyā Indian J. Stat.* **1946**, 401 (1946).
56. Bengtsson, I. & Życzkowski, K. *Geometry of Quantum States: An Introduction to Quantum Entanglement* (Cambridge University Press, 2017).

57. Gessner, M. & Smerzi, A. Statistical speed of quantum states: Generalized quantum Fisher information and Schatten speed. *Phys. Rev. A* **97**, 022109 (2018).
58. Braunstein, S. L. & Caves, C. M. Statistical distance and the geometry of quantum states. *Phys. Rev. Lett.* **72**, 3439 (1994).
59. Liu, J., Yuan, H., Lu, X.-M. & Wang, X. Quantum Fisher information matrix and multiparameter estimation. *J. Phys. A: Math. Theor.* **53**, 023001 (2020).
60. Rangani Jahromi, H. & Lo Franco, R. Hilbert-Schmidt speed as an efficient figure of merit for quantum estimation of phase encoded into the initial state of open n-qubit systems. *Sci. Rep.* **11**, 7128 (2021).
61. Ozawa, M. Entanglement measures and the Hilbert-Schmidt distance. *Phys. Lett. A* **268**, 158 (2000).
62. Luo, S. & Zhang, Q. Informational distance on quantum-state space. *Phys. Rev. A* **69**, 032106 (2004).
63. Paris, M. G. Quantum estimation for quantum technology. *Int. J. Quant. Inf.* **7**, 125 (2009).
64. Jahromi, H. R. & Franco, R. L. Hilbert-Schmidt speed as an efficient figure of merit for quantum estimation of phase encoded into the initial state of open n-qubit systems. *Sci. Rep.* **11**, 85 (2021).
65. Vasile, R., Maniscalco, S., Paris, M. G., Breuer, H.-P. & Piilo, J. Quantifying non-Markovianity of continuous-variable Gaussian dynamical maps. *Phys. Rev. A* **84**, 052118 (2011).
66. Bures, D. An extension of Kakutani's theorem on infinite product measures to the tensor product of semifinite W^* -algebras. *Trans. Am. Math. Soc.* **135**, 199 (1969).
67. Uhlmann, A. The "transition probability in the state space of a*-algebra. *Rep. Math. Phys.* **9**, 273 (1976).
68. Jozsa, R. Fidelity for mixed quantum states. *J. Modern Opt.* **41**, 2315 (1994).
69. Lambert, J. & Sørensen, E. From classical to quantum information geometry: A guide for physicists. *New J. Phys.* **25**, 081201 (2023).
70. Chattopadhyay, A., Chattopadhyay, A. K. & B-Rao, C. Bhattacharyya's distance measure as a precursor of genetic distance measures. *J. Biosci.* **29**, 135 (2004).
71. Mirkin, N., Toscano, F. & Wisniacki, D. A. Quantum-speed-limit bounds in an open quantum evolution. *Phys. Rev. A* **94**, 052125 (2016).
72. Liu, H.-B., Yang, W., An, J.-H. & Xu, Z.-Y. Mechanism for quantum speedup in open quantum systems. *Phys. Rev. A* **93**, 020105 (2016).
73. Ahansaz, B. & Ektesabi, A. Quantum speedup, non-Markovianity and formation of bound state. *Sci. Rep.* **9**, 14946 (2019).
74. Wu, S.-X. & Yu, C.-S. Quantum speed limit for a mixed initial state. *Phys. Rev. A* **98**, 042132 (2018).
75. Zou, H.-M., Liu, R., Long, D., Yang, J. & Lin, D. Ohmic reservoir-based non-Markovianity and quantum speed limit time. *Phys. Scr.* **95**, 085105 (2020).
76. Haseli, S., Salimi, S. & Khorashad, A. A measure of non-Markovianity for unital quantum dynamical maps. *Quant. Inf. Process.* **14**, 3581 (2015).
77. Scully, M. O. *et al.* *Quantum Optics* (Cambridge University Press, 1997).
78. Hosseiny, S. M., Jahromi, H. R. & Amniat-Talab, M. Monitoring variations of refractive index via Hilbert-Schmidt speed and applying this phenomenon to improve quantum metrology *Journal of Physics B: Atomic, Mol. Opt. Phys.* **56**, 175402 (2023).
79. Hosseiny, S. M., Seyed-Yazdi, J. & Norouzi, M. Faithful quantum teleportation through common and independent qubit-noise configurations and multi-parameter estimation in the output of teleported state. *AVS Quant. Sci.* **6**, 856 (2024).
80. Golkar, S. & Tavassoly, M. Dynamics and maintenance of bipartite entanglement via the Stark shift effect inside dissipative reservoirs. *Laser Phys. Lett.* **15**, 035205 (2018).
81. Chandra, N. K., Sk, R. & Panigrahi, P. K. Preservation and enhancement of quantum correlations under Stark effect. *J. Mod. Opt.* **70**, 232 (2023).
82. Puri, R. & Bullough, R. JOSA B Quantum electrodynamics of an atom making two-photon transitions in an ideal cavity. *JOSA B* **5**, 2021 (1988).
83. Dalton, B., Barnett, S. M. & Garraway, B. M. Theory of pseudomodes in quantum optical processes. *Phys. Rev. A* **64**, 053813 (2001).
84. Wootters, W. K. Entanglement of formation of an arbitrary state of two qubits. *Phys. Rev. Lett.* **80**, 2245 (1998).

Author contributions

Practical research was conducted by S.M.H. and M.N. Interpretations and comparison of results and writing of the article were done by S.M.H. and M.N. with the help of J.S.Y. The article was reviewed and edited by J.S.Y.

Competing Interests

The authors declare no competing interests.

Additional information

Correspondence and requests for materials should be addressed to S.M.H. or J.S.-Y.

Reprints and permissions information is available at www.nature.com/reprints.

Publisher's note Springer Nature remains neutral with regard to jurisdictional claims in published maps and institutional affiliations.

Open Access This article is licensed under a Creative Commons Attribution-NonCommercial-NoDerivatives 4.0 International License, which permits any non-commercial use, sharing, distribution and reproduction in any medium or format, as long as you give appropriate credit to the original author(s) and the source, provide a link to the Creative Commons licence, and indicate if you modified the licensed material. You do not have permission under this licence to share adapted material derived from this article or parts of it. The images or other third party material in this article are included in the article's Creative Commons licence, unless indicated otherwise in a credit line to the material. If material is not included in the article's Creative Commons licence and your intended use is not permitted by statutory regulation or exceeds the permitted use, you will need to obtain permission directly from the copyright holder. To view a copy of this licence, visit <http://creativecommons.org/licenses/by-nc-nd/4.0/>.

© The Author(s) 2024